Enhancing the Efficiency and Schedule of Solar Thermal Power Plants by Utilizing Thermal Storage Devices to Minimize Carbon Emissions

P Lingeswaran[1*], Shailendra Kumar Yadav[2], L Ganesh Babu[3], D Magesh Babu[4], Anand Karuppannan[5], Beporam Iftekhar Hussain[6], and S Nanthakumar[7]

[1]Department of Mechanical Engineering, Shree Venkateshwara Hi-Tech Engineering College, Gobichettipalayam 638 455, Tamil Nadu, India
[2]Department of Mechanical Engineering, United College of Engineering and Research, Prayagraj 211010, Uttar Pradesh, India
[3]Department of Robotics and Automation, Rajalakshmi Engineering College, Chennai 602 105, Tamil Nadu, India
[4]Department of Mechatronics Engineering, Velammal Institute of Technology, Panjetty 601 204, Tamil Nadu, India
[5]Department of Electronics and Communication Engineering, Gnanamani College of Technology, Namakkal 637 018, Tamil Nadu, India
[6]Department of Mechanical Engineering, Bapatla Engineering College, Bapatla 522 102, Andhra Pradesh, India
[7]Department of Mechanical Engineering, PSG Institute of Technology and Applied Research, Coimbatore 641062, Tamil Nadu, India

Abstract. The renewable energy method of photo thermal power generation has great promise for future advancements. The core structure and characteristics of energy flow of photo thermal power plants are often overlooked when operating and scheduling these facilities. This paper details the architecture of a Photo Thermal Power Plant (PTPP) with a Thermal Storage System (TSS) and examines the primary energy flow patterns of the plant in order to develop a schedule optimization model for the facility that runs autonomously and generates no carbon emissions. The results of the simulation showed that the photovoltaic power plant's power output capacity and revenue may be improved by adding a TSS to the self-operating model that was originally developed for planning power generation and peak valley energy pricing. When the capacity of the TSS was more than 6 hours, there was no fine for inadequate power generation in the simulation. A rise of 84.9 % in revenue was achieved by increasing the Thermal Storage (TS) system's capacity. Carbon emissions dropped from 26.4×10^3 tons to 22.1×10^3 tons and the overall operating cost went down from 136531.02 k ₹ to 102247.98 k ₹ when the capacity of the TSS went enhanced from 0 to 8 hours. In comparison to previous research, this study's exhaustive optimization model and analysis of energy flows yields a more thorough and rigorous response. Improving the long-term viability of renewable energy sources, developing more efficient energy systems, and developing new clean energy technologies are primary goals of this study.

*Corresponding author : plinges.waran@gmail.com

© The Authors, published by EDP Sciences. This is an open access article distributed under the terms of the Creative Commons Attribution License 4.0 (https://creativecommons.org/licenses/by/4.0/).

1 Introduction

The worldwide energy problem and climate change have united scientists, engineers, and lawmakers in the shared challenge of developing low-carbon energy solutions [1, 2]. Photo Thermal Power Plants (PTPPs) are highly esteemed for their ability to convert solar radiation into electrical energy, due to the clean and abundant solar energy [3]. Combining photovoltaic power generation with concentrated solar power generation, known as PPG, is a developing method for producing large-scale solar electricity. Photo thermal power generation differs from conventional thermal power in that it uses light to generate heat. Instead of using fossil fuels to generate heat as done in conventional thermal power plants, PPG concentrates sunlight onto a collector using a focusing mirror [4]. The traditional method of converting solar energy into electricity is known as photovoltaic power plants (PVPP). The output of the PVPP is unpredictable due to operational weather conditions including day-night alternation and rain [5, 6]. First, the study delves into the basic construction of photo thermal power plants, then it examines the PTPP's interior structure and flow of energy features (IEFCs), and finally it develops a model for PTPP self-running using LCSO. By enhancing the scheduling mechanism of photo thermal power plants, this research aims to increase their automation, adaptability, and low-carbon efficiency. Its long-term goal is to pave the way for cleaner, more sustainable energy by making significant contributions to the creation of such systems. Photo thermal power generation is a technique that harnesses solar radiation to produce electricity, offering numerous benefits in the realms of renewable energy and environmental conservation. Utilizing solar energy can decrease reliance on finite resources and minimize adverse effects on the environment. Many researchers have undertaken thorough research on PPG-related content. To overcome the drawback of solar energy being useful only on sunny days, the authors compared and contrasted photovoltaic power generation with photo thermal power generation coupled with TES [7]. Simulation in the absence of sunshine shown that combining PPG with TES can significantly enhance energy storage duration, offering a novel way to address constraints in solar energy utilization. The recent advancements in PPG and different energy integration solutions in light of the fast growth of PPG investigated by authors [8]. Combining PPG with fossil fuels can better manage the variability of solar energy than using PPG alone, leading to cost savings in PTPP and increased power generation. A high-precision measuring method for focusing mirrors in photovoltaic power generation to enhance efficiency and power output by improving instrument accuracy presented by authors [9, 10]. Integrates PPG systems with photovoltaic power generating systems and Thermal energy storage to tackle the price problem of photo thermal power generation developed by authors [11]. The evaluation methodology for hybrid systems was developed to gather valuable data for designing hybrid power systems and lowering power generation expenses. A photo thermal power plant is a facility that uses solar energy to generate electricity. The system harnesses solar radiation to produce thermal energy, which is then utilized to create steam for powering a generator that produces electricity. PTPP offers benefits such as utilizing renewable energy, emitting little carbon, maintaining consistent performance, and having multifunctional uses. Consequently, numerous scholars are drawn to do research on it. Applying information gap decision-making theory to the problem of solar energy uncertainty management allowed the PTPP to operate optimally. This framework can generate the most efficient selling curve to sell electricity in the electrical market, leading to higher anticipated profits. Currently, there are optimization issues in the scheduling and operation of PTPP, such as cost optimization and power generation optimization. The intricate energy pairing connection and basic structural components of PTPPs have been largely ignored in academic studies. This work suggests a photo thermal power plant self-running LCSO model that includes internal energy flow characteristics. This research comprehensively analyzes the economic and technical

characteristics of every module in a Photo thermal power plant, including the nonlinear elements of thermoelectric productivity in the power generating module, demonstrating innovation.

2 Establishment of LCSO model for photo thermal power plant self-transport containing TSS

The goal of this section is to reduce fuel costs, carbon emission costs, and power shortage penalties in power systems that use photo thermal power plants by analyzing their basic framework, creating a self-operating model of PTPP, and establishing an LCSO model.

2.1 An analysis of the IEFC of a PTPP

There is a lack of a suitable description of the flow of energy features of PP in standard power plant operation models. This includes photo thermal power plants. Studying the IEFCs of PTPP is crucial prior to building the operational model of the photo thermal power plant. A photo thermal power plant's fundamental design is highly dependent on the features of its energy flow. PTPP is made up of standalone energy modules. There are three main types of energy components: thermal energy storage, Solar Field (SF), and Power Block (PB). Different components serve different purposes. Furthermore, PTPP incorporates an energy transfer mechanism known as the Heat Transfer System (HTS) [12, 13]. Fig. 1 displays the internal structure of Photo thermal power plant, illustrating the interconnection between different components.

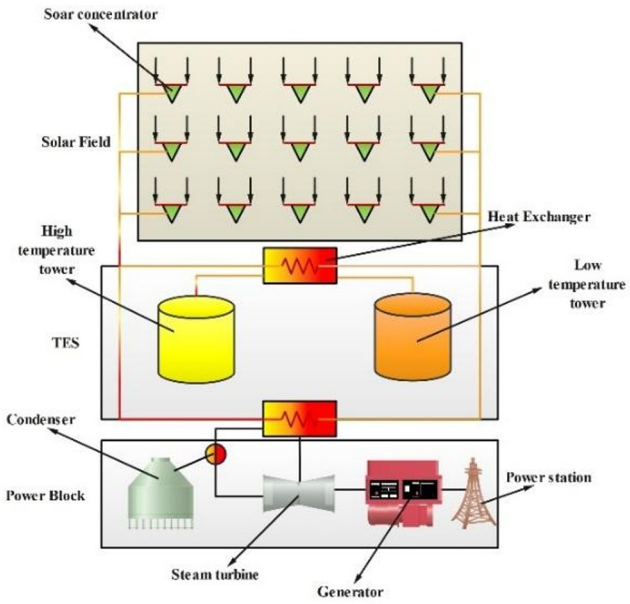

Fig. 1. An illustration the interior structure of the PTPP.

Fig. 1 shows that the heat transfer system's ability to transfer heat between the thermal energy storage, SF, and power block modules is dependent on the cyclical movement of the thermal conductivity of the medium. Solar Furnaces (SFs) use concentrating mirrors to gather solar radiation, which is subsequently transformed into thermal energy then stored in a heat-

conducting standard. The Power Block or the TES are both suitable locations for inserting the thermally conductive material. The heat exchanger in the Power Block is responsible for converting heat energy into steam at extremely high temperatures and pressures. Later on, the turbine and generator of the power plant receive this steam. Even when the sun isn't shining, thermal energy storage can still transfer heat from a storage media to a Power Block. This work determined the internal energy flow process of heating electrons by analyzing their basic internal structure, as depicted in Fig. 2. Fig. 2 displays the conversion of solar radiation power P^{DNI} to output thermal power P^{sf} by Solar Field for the thermal medium. The power system flow (P^{SF}) can be subdivided into heat storage power (P^{chg}) directed towards thermal energy storage (TES) and power generating power (P^{pb}) directed towards Power Block. Energy in the TES system moves towards the Power Block (PB) as exothermic power P^{dsg}, which is then converted into electricity P^{csp} by the Power Block. The energy storage, transmission, and alternate techniques all cause a particular amount of dissipation in all three modules.

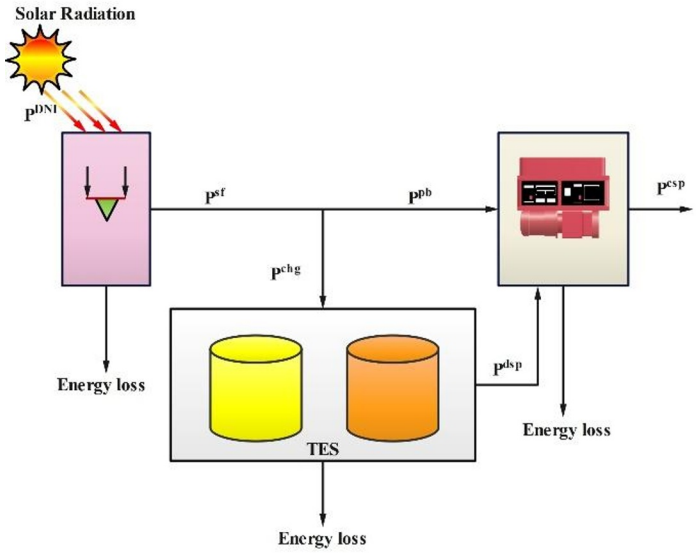

Fig. 2. An illustration of the energy flow within the Photothermal power plant.

During the functioning of a heating power plant, every component experience various operational stage. The six main types of energy flow patterns found in thermal power plants are as follows, according to this study:

- M1 - heat collection (HC) and storaging system
- M2 - HC, storaging, and generation of power
- M3 - HC and generation of power
- M4 - HC, releasing, and generation of power
- M5 - heat releasing and generation of power
- M6 - all optimum modes

The power generating module becomes dormant during M1 because all of the energy from the Solar Field module is directed to the TES during the early morning, when solar radiation is limited [14, 15]. M2 usually takes place during midday, when the solar radiation is at its strongest, with some of the energy transferred to TES and some to Power Block from Solar Field. M3 typically absorbs the energy transferred from the SF to the PB around midday when the solar radiation is at a moderate level. During the evening, the lighting is typically set at M4, increases to M5 during peak evening hours, then switches to M6 for nighttime and

cloudy days. Photo thermal power plants can adaptively switch between two modes to optimize power generation efficiency in response to variations in solar radiation and grid request.

2.2 Photo thermal power plant self-running model and objective procedure construction

Three operational models are developed for each module in this study. An equation representing the total solar radiation power of Photo thermal power plant throughout period t is defined as Equation (1) [16].

$$P_t^{\mathrm{DNI}} = A_{\mathrm{sf}} x_t^{\mathrm{DNI}} \tag{1}$$

A_{sf} in Eq. (1) denotes the surface area of the spotlight mirror in SF. x_t^{DNI} stands for the typical direct solar radiation intensity at time t. The thermal power P_t^{solar} of SF during time t can be found in Equation (2) [17].

$$P_t^{\mathrm{solar}} = \eta_{\mathrm{m}} \eta_{\mathrm{r}} P_t^{\mathrm{DNI}} = \eta_{\mathrm{sf}} P_t^{\mathrm{DNI}} \tag{2}$$

The mirror reflection efficiency is represented by η^{m} in Eq. (2). The receiver's conversion efficiency is denoted by η^{r}. The total photothermal efficiency of the SF module is denoted by η^{sf}. In most cases, the value of the available thermal power and the output thermal power P_t^{sf} of SF are identical. Having said that, SF will experience energy loss at extreme levels of solar radiation. According to Eq. (3), the result thermal power of SF is increased by heat rejection power in this study [18].

$$P_t^{\mathrm{sf}} = P_t^{\mathrm{solar}} - P_t^{\mathrm{CoS}} \tag{3}$$

Eq. (3) defines the heating power as P_t^{CoS} during time period t. The TS stage, E_t of a Thermal Energy Storage (TES) system at time t is influenced by several elements such as thermal storage power, P_t^{chg}, heat release power, P_t^{dsg}, and the prior TS level, E_{t-1}. Equation (4) represents the energy balance equation of Thermal Energy Storage [19].

$$E_t = (1-\eta_{\mathrm{e}}) E_{t-1} + \left(\eta_{\mathrm{c}} P_t^{\mathrm{chg}} - \frac{P_t^{\mathrm{dsg}}}{\eta_{\mathrm{d}}}\right) \Delta t \tag{4}$$

Eq. (4) defines ηe. as the heat dissipation coefficient of Thermal Energy Storage over time interval Δt, whereas ηc and ηd reflect the TS effectiveness and heat release efficiency of Thermal Energy Storage. Eq. (5) sets a limit on the heat transfer rate, which in turn restricts the heat release power and thermal storage power of the Thermal Energy Storage system [20].

$$\begin{cases} 0 \le P_t^{\mathrm{chg}} \le y_t^{\mathrm{chg}} \cdot P_{\max}^{\mathrm{chg}} \\ 0 \le P_t^{\mathrm{dsg}} \le y_t^{\mathrm{dsg}} \cdot P_{\max}^{\mathrm{dsg}} \end{cases} \tag{5}$$

Equation (5) includes $P_{\max}^{\mathrm{chg}}$ and y_t^{chg} as maximum thermal storage power and binary auxiliary variables for TS. $P_{\max}^{\mathrm{dsg}}$ and y_t^{dsg} are max heat release power and binary auxiliary variables representing heat release. Equation (6) shows that the single flow property of the medium limits the operational mode of Thermal Energy Storage, which can be either heat release or heat storage idle [21].

$$y_t^{\mathrm{chg}} + y_t^{\mathrm{dsg}} \le 1 \tag{6}$$

Power Block use the steam cycle to transform thermal energy into electrical energy. Eq (7) is the thermal power (TP) balance equation for this process [22].

$$P_t^{\mathrm{pb}} = P_t^{\mathrm{ST}} + r_t^{\mathrm{pb}} P_{\mathrm{SU}}^{\mathrm{pb}} \tag{7}$$

Equation (7) defines many parameters :P_t^{STT} as the TP utilized for generation of power at time t, P_t^{pb} as the TP of Power Block at time t, $P_{\mathrm{SU}}^{\mathrm{pb}}$ as the TP consumption of Power Block, and r_t^{pb} as a binary auxiliary variable. Power Block restrictions are intricate and encompass

logical relationship constraints, operational constraints, and hotspot transformation efficiency constraints as detailed in Table 1.

Table 1. Limitations of Power Block module.

Criteria	Branch Constrained	Equations
Non-run constraint	Efficiency constraints of thermoelectric conversion	$P_t^{\mathrm{csp}} = \eta_{\mathrm{pb}} P_t^{st}$
	Logical relation constraint	$u_t^{\mathrm{pb}} - u_{t-1}^{\mathrm{pb}} \le r_t^{\mathrm{pb}} \le \frac{\left(1 + u_t^{\mathrm{pb}} - u_{t-1}^{\mathrm{pb}}\right)}{2}$
Run constraint	Max and min output constraints	$u_t^{\mathrm{pb}} p_{\min}^{\mathrm{csp}} \le P_t^{\mathrm{csp}} \le u_t^{\mathrm{pb}} p_{\max}^{\mathrm{csp}}$
	Climb up and down constraints	$-R_{\mathrm{down}}^{\mathrm{csp}} \Delta t \le P_t^{\mathrm{csp}} - P_{t-1}^{\mathrm{csp}} \le R_{\mathrm{up}}^{\mathrm{csp}} \Delta t$
	Minimum downtime constraints	$\sum_{\tau=t-T_{\mathrm{off}}^{\mathrm{pb}}}^{t-1} \left(1 - u_\tau^{\mathrm{pb}}\right) \ge T_{\mathrm{off}}^{\mathrm{pb}} \left(u_t^{\mathrm{pb}} - u_{t-1}^{\mathrm{pb}}\right)$
	Minimum boot time constraint	$\sum_{\tau=t-T_{\mathrm{on}}^{\mathrm{pb}}}^{t-1} u_\tau^{\mathrm{pb}} \ge T_{\mathrm{on}}^{\mathrm{pb}} \left(u_{t-1}^{\mathrm{pb}} - u_t^{\mathrm{pb}}\right)$

Table 1 defines u_t^{pb} and u_{t-1}^{pb} as binary variables indicating the starting and shutdown condition of PB at time t and $t-1$, individually. When the range at 1, they signify creation, and when they are not, they signify shutdown. P_t^{csp} reflects the power output of Photo thermal power plant during period t. η_{pb} denotes the thermal effectiveness of the PB. $P_{\min}^{\mathrm{csp}}$ and $P_{\max}^{\mathrm{csp}}$ indicate the lowest and highest technical production levels of the PB generator set, respectively. The $R_{\mathrm{down}}^{\mathrm{csp}}$ and $R_{\mathrm{up}}^{\mathrm{csp}}$ indicate the descending and ascending speeds of the generator set, respectively. $T_{\mathrm{on}}^{\mathrm{pb}}$ and $T_{\mathrm{off}}^{\mathrm{pb}}$ depict the minimum time mandatory for Power Block to start up and shut down, respectively. Both the starting and ending states of the Power Block module are guaranteed to be coherent by the logical relation constraint. The technical requirements are satisfied since the effectiveness limit of thermoelectric conversion guarantees that thermal energy may be converted into electrical energy. Operational constraints refer to the restrictions on Power Block modules during operation, including the maximum and minimum result power levels and thermal power consumption, in order to ensure security and effectiveness. For the purpose of balancing supply and demand on the grid, the output limitations establish maximum and minimum power output for the PB module. To prevent grid instability or equipment damage, Power Block modules can only adjust result power at a certain speed, which is limited by ascending and descending constraints. Power Block components are engineered to minimize startup time and down time. The thermal energy transfer among the three modules of Photo thermal power plant follows the principle of energy conservation, as demonstrated in Equation (8) [23].

$$P_t^{\mathrm{sf}} + P_t^{\mathrm{dsg}} = P_t^{\mathrm{chg}} + P_t^{\mathrm{pb}} \tag{8}$$

This research sets two self-operating objectives for PTPP. The initial objective is to focus on the power generating plan. This involves PTPP adjusting its operating strategy based on the plan received from the power grid dispatch center. The objective function is represented by Equation (9) [24].

$$\begin{cases} \min F^{\mathrm{sche}} = \sum_{t=1}^{T} \pi_t^{\mathrm{vio}} \Delta P_t^{\mathrm{vio}} \Delta t \\ \Delta P_t^{\mathrm{vio}} = \begin{cases} P_t^{\mathrm{sche}} - P_t^{\mathrm{csp}}, P_t^{\mathrm{csp}} < P_t^{\mathrm{sche}} \\ 0, P_t^{\mathrm{csp}} > P_t^{\mathrm{sche}} \end{cases} \end{cases} \tag{9}$$

Eq. (9) defines F^{sche} as the fine for not following the power generating plan, and π_t^{vio} as the penalty factor for not adhering to the plan during time period t. $\Delta P_t^{\mathrm{vio}}$ denotes the no of violations through time t. P_t^{sche} signifies the intended generation of power result for the t. The second goal is to change the power market such that peak valley electricity costs are

used. PTPP power generation can be adjusted due to the presence of TSS, making Eq. (10) the goal function [25].

$$\max F^{\text{pric}} = \sum_{t=1}^{T} \pi_t^{\text{pric}} P_t^{\text{csp}} \quad (10)$$

Eq. (10) shows that F^{pric} represents the revenue of PTPP, while π_t^{pric} indicates the electricity cost through time t.

2.3 PTPP LCSO model for power systems

Due to the Carbon reduction and electricity effectiveness benefits of photo thermal power production, scheduling cost concerns like fuel price and Carbon emission cost must be considered while designing the power system for photo thermal power generation [26, 27]. Minimizing the operating price, represented as F-oper in Equation (11).

$$\min F^{\text{oper}} = F^{\text{fuel}} + F^{\text{carb}} + F^{\text{curL}} + F^{\text{curS}} \quad (11)$$

Equation (11) breaks down as follows : F^{fuel} signifies fuel cost, F^{carb} denotes the price of Carbon emissions, F^{curL} signifies the fine price for load shedding, and F^{curS} denotes the fine price for inadequate backup. Equation (12) represents the expression for F^{fuel} [28].

$$F^{\text{fuel}} = \sum_{i=1}^{N} \sum_{t=1}^{T} \left[C_i^{\text{fuel}} \cdot f^{\text{fuel}} \left(P_{i,t}^{\text{thm}} \right) + r_{i,t} SU_i \right] \quad (12)$$

In equation (12), N is defined as the sum of all conventional units, and C_i^{fuel} represents the cost per unit of fuel. Unit i, $P_{i,t}^{\text{thm}}$ denotes the result of the i^{th} unit during time t. The binary auxiliary variable $r_{i,t}$. $f^{\text{fuel}}\left(P_{i,t}\right)$ denotes the fuel consumption of the i^{th} unit throughout the t time period. The i^{th} unit's starting price is represented by SU_i. The formula's variables pertain to economic factors in low-carbon scheduling optimization. The goal is to optimize these variables to reduce operating expenses, maintain power supply stability, and adhere to environmental regulations. The definition of F^{carb} is provided in Equation (13) [29].

$$F^{\text{carb}} = \sum_{i=1}^{N} \sum_{t=1}^{T} \left\{ C^{\text{carb}} \left[K_i^{\text{fuel}} \cdot f^{\text{fuel}} \left(P_{i,t}^{\text{thm}} \right) + r_{i,t} SE_i \right] \right\} \quad (13)$$

Eq. (13) defines the cost of CO_2 emissions as C^{carb} .The coefficient of Carbon emission for each unit of the i^{th} fuel unit is represented by K_i^{fuel} .The initial Carbon emissions of the i^{th} unit are represented by the symbol SE_i. Photo thermal power plant must compute its Carbon emission expenses by considering the fuel consumption as well as Carbon emission coefficient of every unit. These charges are then included in the total price for ideal scheduling in order to minimize the environmental impact. Equation (14) represents the expressions of F^{curL} and F^{curs} [30].

$$\begin{cases} F^{\text{curL}} = \sum_{t=1}^{T} C^{\text{curL}} P_t^{\text{curL}} \Delta t \\ F^{\text{curS}} = \sum_{t=1}^{T} C^{\text{curS}} P_t^{\text{curS}} \Delta t \end{cases} \quad (14)$$

Equation (14) shows that the fine coefficients for load shedding and inadequate back up are denoted by C^{curL} and C^{curS} , respectively. P_t^{curL} and P_t^{curS} stand for the load shedding and inadequate backup that occurred during period t, respectively. For standard units, Eq. (15) represents the secondary consumption characteristic curve [31, 32].

$$f^{\text{fuel}} \left(P_{i,t}^{\text{thm}} \right) = a_i \left(P_{i,t} \times P_{i,t} \right) + b_i P_{i,t} + c_i u_{i,t} \quad (15)$$

Eq (15) represents the i^{th} unit's secondary consumption coefficients as a_i, b_i, and c_i. At time t, the i^{th} unit's status is indicated by the binary variable $u_{i,t}$, which can be either turned on or off. The power station scheduler must account for nonlinear traits to optimize the unit's procedure strategy, coordinate start-up, operation, and shutdown, adjust to power grid load changes, and minimize energy discard to enhance operational efficiency and cut costs. The limitations of the low-carbon scheduling optimization model encompass a broad spectrum, as illustrated in Fig. 3.

The output, total number, and index of PTPP and wind farms are shown considered in this research wok. The variables j/w, $N^{\text{csp.}}$ /, N^{wind}, and $P_{j,t}^{\text{csp}}$ /$P_{w,t}^{\text{wind}}$. P_t^{loadF} and R_t^{gridS} represent

the power grid's rotational reserve capacity and load requests at t. The research and the economic benefits of photo thermal power generation, particularly when combined with TES configuration, were emphasized by the authors [33, 34]. This study offers a precise scheduling method by thoroughly examining the interior energy stream of Photo thermal power plant, creating a comprehensive optimization model, and taking into account the nonlinear aspects of thermoelectric effectiveness.

3 Experiment on the PTPP self-sustaining LCSO

In order to understand the impact of TS modules on the self-operation of PTPP in the built autonomous LCSO typical, this analysis used rigorous computational simulations. The research also analyzes how the system's low-carbon scheduling is affected by module capacity as well as light field capacity.

3.1 Constructing a data-driven experimental setting and developing a simulation model

A workstation outfitted with 128 GB of RAM and two 2.4 GHz Intel Xeon E5-2680 processors forms the basis of the simulation computing hardware platform. A 64-bit Windows 7 operating system, the YALMIP toolkit, the MATLAB programming, and the GUROBI solver make up the software environment for simulation calculations. The empirical parameters of the trough PTPP model in the SAM program, which is generated by NREL, were extensively used in the time-thermal power station simulation. Policy restrictions, technological feasibility, environmental effect, and economic feasibility inform the selection of these variables. The outcomes are influenced by these variables: thermal energy storage capacity impacts nighttime power generating capacity, whereas photo thermal transformation efficiency affects energy utilization rate. Operating expenses and electricity rates impact income, whereas carbon expenses are linked to adhering to environmental regulations. The precise data is displayed in Table 2.

Table 2. Details of the PTPP model's technical parameters

Variable type	Value
Hourly heat storage loss (%)	0.03
Rated generating capacity (MW)	110.00
Capacity of the thermal energy storage (h)	4.20
Min technical output (MW)	35.00
Min downtime (h)	2.30
Max technical capacity (MW)	120.00
Climbing speed (MW/h)	85.00
Solar multiple	1.50
Efficiency for Heat storage and release (%)	98.12
Efficiency for Thermo-electric conversion (%)	39.46

Table 2 provides the technical variable settings. There are two possible approaches to creating simulations that can operate independently: In Scenario A, the peak load on the electricity system occurs during the night, whereas in Scenario B, it occurs during the day. In the first scenario, a photo thermal power plant employs heat storage technology to fulfill peak energy demand during the day by releasing stored heat. This scenario is anticipated to showcase PTPP's capability to sustain efficient power generation via TES when sunshine is

not available. Scenario B aims to assess the peak power generating capacity of PTPP under direct sunshine and the effectiveness of solar energy conversion during peak hours. Together, the methods of thermal energy storage for controlling supply demand and storing excess energy and the efficiency of photovoltaic power plants operating in high-radiation environments will be on display in this scenario. The greatest variations in grid demand occur during the day and night during peak load periods. Evaluating the model's performance thoroughly can be achieved by configuring Scenario A, Scenario B. The experimental environment allows for the evaluation of various aspects such as power generation efficiency during periods of intense solar radiation, and scheduling tactic optimization. Additionally, data collection for policymaking purposes is facilitated. By simulating low-carbon scheduling optimization, the IEEE-RTS-96 system is enhanced. Fig. 3 illustrates the self-administering simulation scenario.

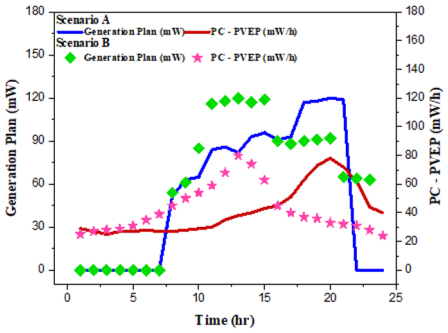

Fig. 3. Scenario for autonomous simulation.

Fig. 3 shows the penalty coefficient peak valley electricity cost, abbreviated as PC-PVEP. Fig. 3 shows that between 18 and 20 hours, and scenario A's power generating scheme both attain its peaks at 120 MW/h and 80 WM, respectively. Between hours 10 and 14, PC-PVEP reaches 120 MW/h and the power generation plan reaches 80 MW, as shown in Fig. 3, in scenario B. As shown in Fig. 4, the simulation results for low-carbon schedule optimization, wind power, and Direct Normal Irradiance (DNI) are shown.

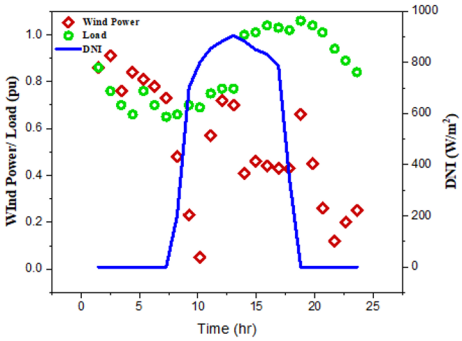

Fig. 4. Simulation of LCSO.

Fig. 4 displays the wind power simulation results at 10 hours, with the lowest value being 0.05 pu. Midday is the peak of the Direct Normal Irradiance (DNI), and the forecast load range is lesser than that at 12 hours. The simulation curve chosen for this research accurately reflects the bulk of real-world practical scenarios.

4 Results of PTPP self-operation analysis

Findings from the study indicate that peak-and-valley cost planning for power generation and the energy market are the two self-operating goals of a photovoltaic power plant. In scenario A, where the simulation runs autonomously, they are referred to as Scheme AI and AII. Autonomous simulation with schemes BI and BII should be run for C. This research examines the PTPP internal thermal power equilibrium using four different approaches. Examining objective - I, as shown in Fig. 5(a) to 5(d), is the initial stage.

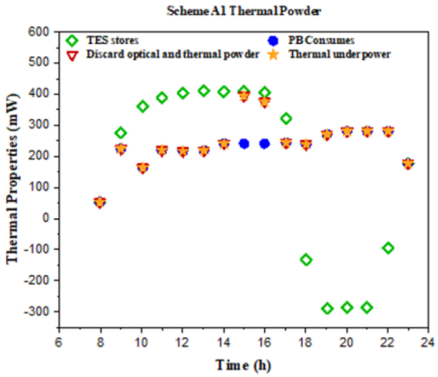

Fig. 5(a). The photo thermal plant's scheme A1 internal thermal power balance in relation to target I

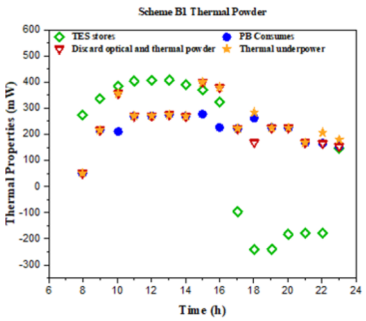

Fig. 5(b). The photo thermal plant's scheme B1 internal thermal power balance in relation to target I

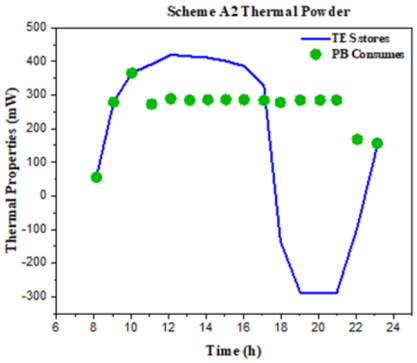

Fig. 5(c). The photo thermal plant's scheme A2 internal thermal power balance in relation to target I

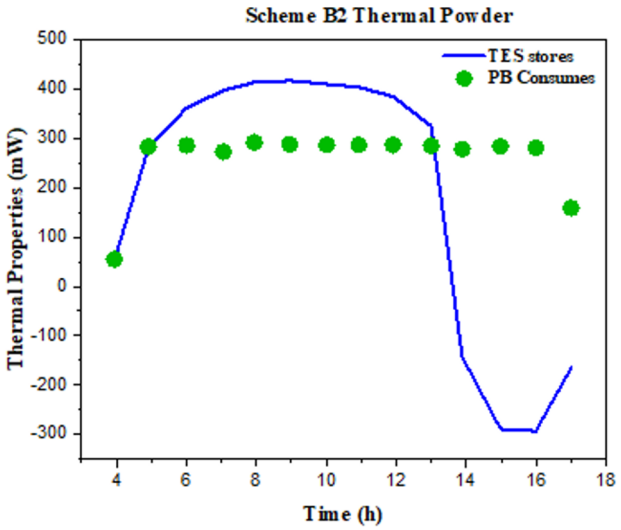

Fig. 5(d). The photo thermal plant's scheme B2 internal thermal power balance in relation to target I

Based on Fig. 5(a), Scheme AI showed thermal power wastage between 14 and 16 hours, suggesting that the production of thermal energy above the required amount. Between 22 and 24 hours, there was a lack of thermal power, indicating that the TES system did not fulfill the heat demand throughout the night. Fig. 5(b) illustrates that Scheme BI's thermal energy administration was effective, as there was minimal thermal power wastage, showcasing the efficiency of its TES heat release and system capacity method. Scheme AII's thermal power station uses a TES module to store heat throughout the day, as seen in Fig. 5(c). The thermal storage module starts releasing heat at around 6'o clock in the evening so it can fulfill the nighttime heat requirement. According to Fig. 5(d), the TPP in Scheme BII begins storing thermal energy in the morning and begins releasing it at 2 pm in order to meet the peak demand in the afternoon and evening. The study examines and discusses how Thermal storage system (TSS) capability affects the self-operation of Photo thermal power plant, with the results displayed in Fig. 6.

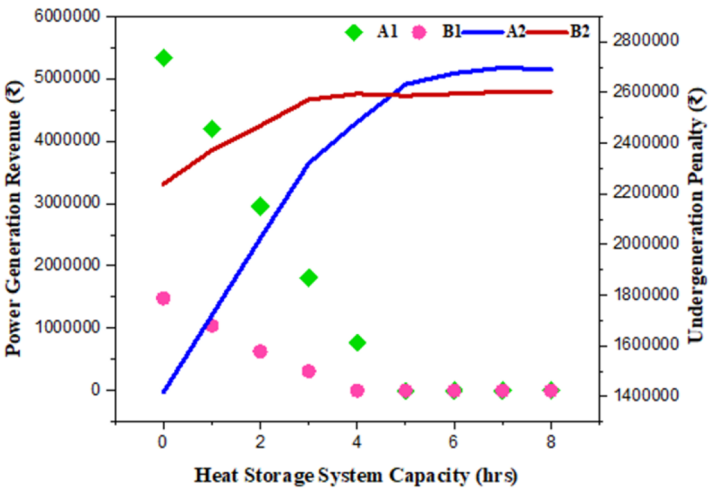

Fig. 6. Self-operational outcomes of a TPP.

Improving AI and BI schemes by increasing the TSS capacity reduces the forfeit for inadequate generating of power (IPDP). For the absence of any thermal storage system capacity, the IPGP of AI is 766229.5 ₹ while that of BI is 310697.2 ₹. At 6 hours of thermal storage system capacity, the IPGP for AI is 0, and at 5 hours of thermal storage system capacity, the IPGP for scheme BI is 0. There is less of a penalty for Scenario B because, in comparison to Scenario A, there is a better match with solar energy resources during the midday. The revenue generation of AII and BII systems can be enhanced by improving TSS capabilities. Scheme AII's power generation revenue increases from ₹34,830 to ₹64,409, a growth of 84.9%, when the TS module capacity is increased from 0 to 6 hours.

4.1 Evaluation of PTPP- LCSO data

This research examines the outcomes of PTPP's low-carbon scheduling from many viewpoints. At various thermal storage system capacities, Table 3 shows the results of comparing technical and economic scheduling indicators. Based on Table 3, the total operating cost drops from 136539.20 k ₹ to 102254.10 k ₹ as the TSS capacity grows from 0 to 8 hours. Additionally, the carbon emissions go down from 26.4×10^2 tons to 22.1×10^4 tons. In order to save costs and carbon emissions, TSS can use stored solar energy to generate electricity at night. Indicators like total operating price show little to no change as the TSS capacity increases between 4 and 8 hours. The 4-hour TSS capacity is adequate to address the issue of uninhibited light, and further expanding the TSS capability does not notably enhance the power generation of Photo thermal power plant. Fig. 7(a) and Fig. 7(b) displays the scheduling plan of Photo thermal power plant with TSS capabilities of 0 hours and 4 hours.

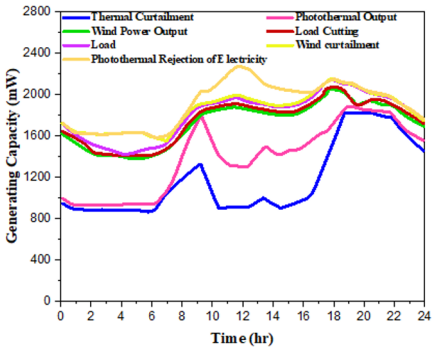

Fig. 7(a). Scheduling plan of photo thermal power plant with TSS capabilities of 0 hours.

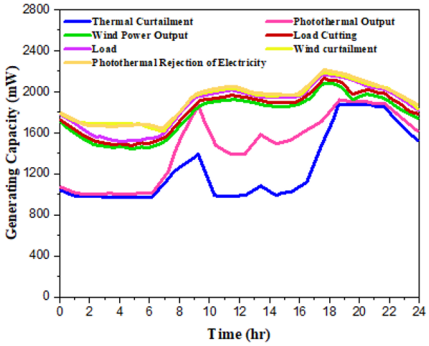

Fig. 7(b). Scheduling plan of photo thermal power plant with TSS capabilities of 4 hours.

Table 3. Comparing economic and technical indicators for dispatching.

Capacity (hours)	0h	2h	4h	6h	8h
Cost for Comprehensive operation (k₹)	137604.6	109771.3	103171.7	103971.4	102403.1
Shearing load (MWh)	129.5	0	0	0	0
Carbon emissions (10^3ton)	27.4	27.2	23.4	23.3	23.1
Light power for Discard (MWh)	1987.5	935.8	0	0	0
Start-stop cost (k₹)	6283.854	4237.124	2165.332	2165.332	2165.332
Generation cost (k₹)	58912.16	56715.06	54593.14	54467.83	54434.42
Wind power (MWh)	926.9	949.7	949.7	949.7	949.7
Inadequate reserve (MWh)	125.4	0	0	0	0

A large quantity of light goes out between the hours of 7 and 17 when the thermal storage system capacity is 0 h in Fig. 7(a), indicating that there is no thermal storage system. At 20:00, when there is no solar radiation, the Photovoltaic Power Plant (PTPP) cannot produce power, leading to system load shedding. In Fig. 7(b), with a Thermal storage system capacity of 4 hours, Photo thermal power plant may generate power continuously during peak nighttime hours, eliminating light curtailment and system load shedding. This work examines how alterations in solar multiples affect Photo thermal power plant scheduling outcomes, as illustrated in Fig. 8(a) to Fig. 8(c). The overall expense decreases with increasing solar multiple in Fig. 8(a). The whole cost drops by about 15.68 % when the thermal storage system's capacity is 8 hours. Emissions of carbon in Fig. 8(b) exhibit an inverse relationship with the solar multiple. Increasing the solar multiple from 1.0 to 2.0 while the Thermal storage system capacity is 8 hours results in a decrease in carbon emissions of around 16.98%. Light abandonment phenomena occur in Fig. 8(c) when the Thermal storage system capacity is 8 hours and the solar several exceeds 2.0, leading to PTPP being restricted by the PB module capacity.

5 Discussions

The model presented in the paper demonstrates favourable economic advantages and possibilities for reducing carbon emissions, but it has limits in terms of its reach and depth. Economic processes in different regulatory and market settings, like changes in power prices, subsidies policies, and renewable energy market competitiveness, are not extensively investigated in the research; instead, the focus is on model creation and optimization. The real economic benefits of the model might be significantly affected by these variables. Furthermore, while the model has made progress in decreasing carbon emissions, the environmental effect assessment lacks comprehensiveness. No prior research has thoroughly examined how PTPP's construction and operation may influence water resource management and biodiversity in the area. The model's shortcomings may restrict its usefulness in different real-world scenarios. Streamlined assumptions can result in an inadequate evaluation of market changes and environmental consequences, thereby influencing decision makers' perception of project advantages. In order to enhance model performance, future research should incorporate more realistic assumptions, merge field tests with updated technology, and investigate the possibilities for integration with other renewable energy sources. Models may encounter technological problems, infrastructure requirements, significant investment expenses, and policy obstacles throughout the implementation phase. The project's implementation will be expedited through the establishment of a system for multiple

stakeholder communication and collaboration. This mechanism will ensure that technological, economic, and environmental factors are considered to develop sustainable energy systems. The increasing integration of renewable energy technologies makes it important to research how recommended models could coexist and be improved with other systems in the future. Hybrid systems improve the grid's consistency and dependability by combining numerous power sources. Future energy that is both sustainable and low-carbon is made possible by advanced scheduling and energy management technologies.

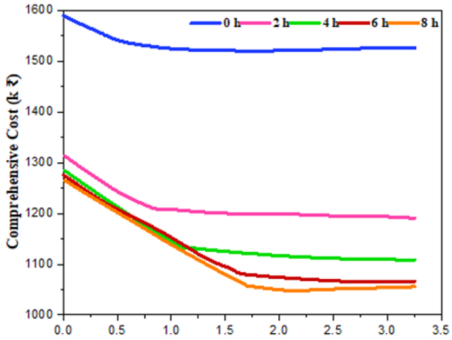

Fig. 8(a). Comparison on the comprehensive cost of the photo thermal power plant.

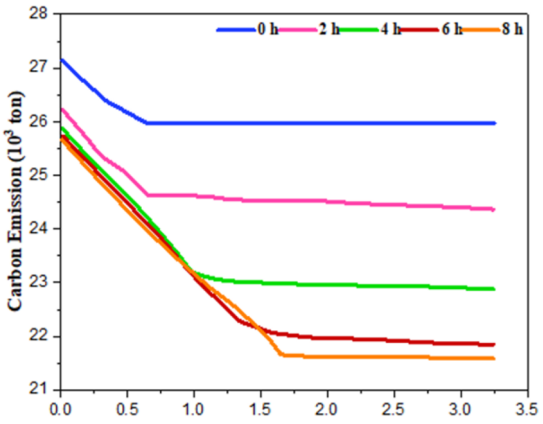

Fig. 8(b). Comparison on the Carbon emission of the photo thermal power plant.

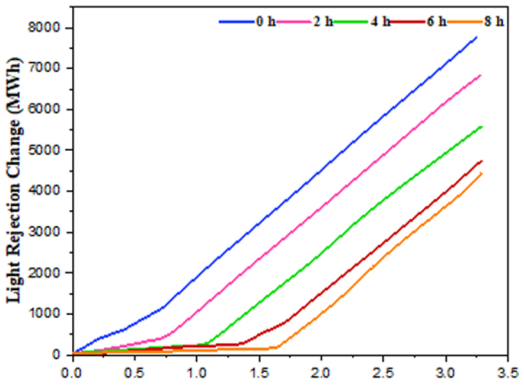

Fig. 8(c). Comparison on the light rejection change of the photo thermal power plant.

6 Conclusions

A self-running LCSO model for internal energy flow characteristics that accounts for PTPP was presented in this article to address the high schedulability of PPG. Each energy module's characteristics and connections were investigated during the building process of the self-running model. A self-executing model served as the foundation for the low-carbon scheduling optimization model, which underwent a preliminary evaluation. Scheme AI had an IPGP of ₹2636521.62 and scheme BI had an IPGP of ₹769239.44, according to the results of the autonomous model's simulations, when the thermal storage system capacity was set at 0 hours. When the time-sharing system capacity reached 6 hours, the individual performance goal percentages of both scenarios dropped to 0%. Increasing the TSS capability between 0 and 6 hours resulted in scheme AII's power generating income rising from ₹2908130.85 to ₹5377829.46, and scheme BII's revenue increasing from ₹4528768.80 to ₹5197722.39. Increasing the TSS capacity from 0 to 8 hours in the LCSO model simulation resulted in a decrease in total operating costs from ₹136531.02k to ₹102247.98k and a decrease in carbon emissions from 26.4×10^3 tons to 22.1×10^3 tons. When the solar multiple surpasses 2.0 and the TSS capacity reaches 8 hours, light abandonment will take place. Currently, Power Block module coordination was necessary to maximize advantages. The study findings suggest that the presence of Thermal storage system can enhance the power generation capability of nocturnal PTPP, aiding in fulfilling power generation targets and boosting PTPP revenue. This work offers theoretical direction for designing and operating PTPP, with practical implications for advancing the progress of clean energy. The study suggests that practitioners and decision-makers of PTPP focus on researching and developing TES, creating supportive policies for technological innovation and investment, and prioritizing environmental protection and social benefits. To advance photo thermal power generation and accomplish a low-carbon energy transition, it is crucial to collaborate across disciplines and plan ahead.

References

1. Y. Cui, P. Zeng, W. Zhong, Z. Wang, P. Zhang, Y. Zhao, Low-carbon Economic Dispatch of Electro-gas-thermal Integrated Energy System Based on Oxy-combustion Technology. Zhongguo Dianji Gongcheng Xuebao/Proceedings of the Chinese Society of Electrical Engineering. **41,** 592 (2021).
2. R. Girimurugan, P. Selvaraju, P. Jeevanandam, M. Vadivukarassi, S. Subhashini, N. Selvam, S. K. Ahammad, S. Mayakannan, S. K. Vaithilingam, Application of Deep Learning to the Prediction of Solar Irradiance through Missing Data. International Journal of Photoenergy. **2023,** (2023).
3. X. Li, R. Zhang, L. Bai, G. Li, T. Jiang, H. Chen, Stochastic low-carbon scheduling with carbon capture power plants and coupon-based demand response. Appl Energy. **210,** 1219 (2018).
4. B. Karthikeyan, G. Praveen Kumar, R. Saravanan, Alberto Coronas, Ramadas Narayanan, R. Girimurugan, Solar powered cascade system for sustainable deep-freezing and power generation - exergoeconomic evaluation and multi-objective optimization for tropical regions. Thermal Science and Engineering Progress. 102552 (2024).
5. M. R. Nayak, P. Praveen, P. S. Teja, K. Kishore, J. Sushma, Electrical energy generation using magnetor. Journal of Advanced Research in Dynamical and Control Systems. **11,** 173 (2019).

6. Y. Akishev, N. Trushkin, M. Grushin, A. Petryakov, V. Karal'nik, E. Kobzev, V. Kholodenko, V. Chugunov, G. Kireev, Y. Rakitsky, I. Irkhina, Inactivation of microorganisms in model biofilms by an atmospheric pressure pulsed non-thermal plasma. Plasma for Bio-Decontamination, Medicine and Food Security. 149 (2011).
7. L. Hetier, J. Poëtte, L. Bastard, J.-F. Roux, P.-B. Vigneron, J. E. Broquin, THz generation by beating of self-running Er-based ion-exchanged DFB lasers co-integrated on one single chip. Integrated Optics: Devices, Materials, and Technologies XXVII. **12424,** 78 (2023).
8. S. Kanjanachuchai and C. Euaruksakul, Self-running Ga droplets on GaAs (111) A and (111) B surfaces. ACS Appl Mater Interfaces. **5,** 7709 (2013).
9. X. Wu, Q. Cui, Multi-objective flexible flow shop scheduling problem with renewable energy. Jisuanji Jicheng Zhizao Xitong/Computer Integrated Manufacturing Systems. **24,** 2792 (2018).
10. S. Eswaran, M. Chandru, M. Vairavel, R. Girimurugan, Numerical Study on Solar Water Heater using CFD Analysis. International Journal of Engineering Sciences & Research Technology. **3,** 1485 (2014).
11. J. Hu, X. Wang, C. Jiang, H. Cong, Low-carbon Economic Dispatch of Power System Considering Participation of Integrated Energy Service Providers. Dianwang Jishu/Power System Technology. **44,** 514 (2020).
12. Ganesan, Sakthivel, Prince Winston David, Pravin Murugesan, Praveen Kumar Balachandran. Solar photovoltaic system performance improvement using a new fault identification technique. Electric Power Components and Systems. **52,** 42 (2024).
13. Z. Lu, H. Liu, L. He, Low-carbon Economic Dispatch of Integrated Electricity and Natural Gas Systems Considering Period Granulation. Quanqiu Nengyuan Hulianwang. **2,** 266 (2019).
14. Prasanth Ponnusamy, S Seenivasan, G Ravivarman, K Sathiyasekar, Ramasamy Girimurugan, Experimental Analysis of Phase Change Materials Supported with Hemp-Stem-Derived Biochar for Enhanced Solar-Thermal Energy Conversion and Storage. IGI Global. 177 (2024).
15. H. Yang, Q. Zheng, G. Liu, J. Guo, Low-carbon scheduling in permutation flow shop problem by differential genetic algorithm. Zhongnan Daxue Xuebao (Ziran Kexue Ban)/Journal of Central South University (Science and Technology). **44,** 4554 (2013).
16. L. Yin, X. Li, L. Gao, C. Lu, Z. Zhang, A novel mathematical model and multi-objective method for the low-carbon flexible job shop scheduling problem. Sustainable Computing: Informatics and Systems. **13,** 15 (2017).
17. Ganesan, Sakthivel, Prince Winston David, Praveen Kumar Balachandran, Ilhami Colak, Power enhancement in PV arrays under partial shaded conditions with different array configuration. Heliyon **10,** (2024).
18. K Kannakumar, A Murugesan, S Balasubramani, Ramasamy Girimurugan, Achintya Sharma, Enhancing Desalination and Liquid Desiccant Regeneration Efficiency Through a Hybrid Solar Still: A Comparative Study with Steel Scrap Thermal Storage. IGI Global. 133 (2024).
19. H. Chen, W. Mao, R. Zhang, W. Yu, Low-carbon optimal scheduling of a power system source-load considering coordination based on carbon emission flow theory. Dianli Xitong Baohu yu Kongzhi/Power System Protection and Control. **49,** 1 (2021).
20. Manoj Kumar Shanmugam, S Sathishkumar, GB Mohankumar, Ramasamy Girimurugan, Achintya Sharma, Improving Solar Still Performance with Porites Coral Biomaterial: A Comparative Study on Enhanced Efficiency. IGI Global. 283 (2024).

21. Murugesan, Palpandian, Prince Winston David, Rajvikram Madurai Elavarasan, G. M. Shafiullah, Praveen Kumar Balachandran. A jigsaw puzzle-based reconfiguration technique for enhancing maximum power in partially shaded hybrid photovoltaic array implementation. In Green energy systems. 223 (2023).
22. Y. Cui, G. Deng, Z. Wang, M. Wang, Y. Zhao, Low-carbon economic scheduling strategy for power system with concentrated solar power plant and wind power considering carbon trading. Dianli Zidonghua Shebei/Electric Power Automation Equipment. **41,** 232 (2021).
23. H. Liu, S. Nie, Low carbon scheduling optimization of flexible integrated energy system considering CVaR and energy efficiency. Sustainability (Switzerland). **11,** (2019).
24. Srilakshmi, Koganti, Sravanthy Gaddameedhi, Subba Reddy Borra, Praveen Kumar Balachandran, Ganesh Prasad Reddy, Aravindhababu Palanivelu, Shitharth Selvarajan. Optimal design of solar/wind/battery and EV fed UPQC for power quality and power flow management using enhanced most valuable player algorithm. Frontiers in Energy Research **11,** 1342085 (2024).
25. D. W. Seng, J. W. Li, X. J. Fang, X. F. Zhang, J. Chen, Low-carbon flexible job-shop scheduling based on improved nondominated sorting genetic algorithm-II. International Journal of Simulation Modelling. **17,** 712 (2018).
26. J. Sun, Self-operation and low-carbon scheduling optimization of solar thermal power plants with thermal storage systems. Energy Informatics. **7,** (2024).
27. R. Jayaraman, A. Sivalingam, S. Rahul, V. Prabaharan, S. Nanthakumar, Sk Hasane Ahammad, R. Girimurugan, Square Pyramid and Single Slope Solar Still: Experimental Analysis for Various Depth of Water. Scientific and Technological Advances in Materials for Energy Storage and Conversions: Select Proceedings of FLUTE 2023. 29 (2024).
28. J. Zhao, L. Hua, Variable frequency energy-saving analysis of city heat power station heating system. Advanced Materials Research. 1319 (2012).
29. X. Zhu, S. Zhu, S. Guo, A study of predictive control of energy-saving of heating process. Advanced Materials Research. 1810 (2011).
30. Z. Liu, Q. Luo, L. Wang, H. Tang, Y. Li, The Low-Carbon Scheduling Optimization of Integrated Multispeed Flexible Manufacturing and Multi-AGV Transportation. Processes. **10,** (2022).
31. Y. Liao, J. Chen, Y. Yang, Optimal Scheduling of Virtual Power Plant with P2G and Photo-Thermal Power Plant Considering the Flexible Operation of Carbon Capture Power Plants. Dianli Jianshe/Electric Power Construction. **43,** 20 (2022).
32. Krishnamoorthy, Murugaperumal, P. Ajay-D-Vimal Raj, N. P. Subramaniam, M. Sudhakaran, and Arulselvi Ramasamy. "Design and development of optimal and deep-learning-based demand response technologies for residential hybrid Renewable Energy Management System." *Sustainability* 15, no. 18 (2023): 13773.
33. F. Tian, Internet of Things Temperature Control of Indirect Dual Tank Heat Storage System in Solar Photo-Thermal Power Plant. Thermal Science. **28,** 1477 (2024).
34. E. S. Svendsen, A. Hafner, H. Selvnes, K. N. Widell, Energy flow analysis of a poultry processing plant. Refrigeration Science and Technology. 13 (2020).